日本建築学会構造系論文集 第81巻 第721号, 447-457, 2016年3月
J. Struct. Constr. Eng., AIJ, Vol. 81 No. 721, 447-457, Mar., 2016
DOI http://doi.org/10.3130/aijs.81.447

EFFECT OF ROCKING FOUNDATION INPUT MOTION ON THE INELASTIC BEHAVIOR OF STRUCTURES

基礎入力動の回転成分が上部建物の地震時挙動に与える影響

*Oguz Can OGUT**, Masafumi MORI*** and Nobuo FUKUWA****
オグトゥ オグズジャン, 護　雅史, 福和伸夫

A parametric study is applied to determine the effects of rocking foundation input motion (RFIM) on the nonlinear behavior of SDOF elasto-plastic structure considering soil-structure interaction (SSI). A new lumped parameter model considering SSI is constructed based on the results of the thin layer method (TLM) for different embedment ratios of foundations taking place on homogeneous elastic half-space. After that the soil-structure model is analyzed under some earthquake records. Consequently, it is claimed that by increasing ductility factor values, the effect of RFIM becomes more important especially for high-rise buildings having deep embedment ratios. The reason of this phenomena is considered that equivalent elastic stiffness of superstructure becomes softer for increasing values of ductility capacity, therefore the additional force coming from the rocking input motion becomes more important than inertial interaction for the response of the superstructure.

Keywords : *Soil-structure interaction, Nonlinear structural analysis, Lumped parameter models, Foundation input motion, Ductility factor, Embedded foundation*
動的相互作用, 非線形解析, 質点系モデル, 基礎入力動, 塑性率, 根入れ基礎

1. Introduction

To determine the damage to structures during large earthquakes, soil-structure interaction (SSI) becomes very important in some situations especially for low and middle rise buildings. Therefore, researches on this topic are necessary for earthquake resistance design to understand the key parameters of SSI that influence on inelastic behavior of superstructures.

As it is known, the effect can be analyzed under the subtopics named as kinematic interaction (KI) which occurs due to rigidity differences of foundations and the surrounding soil, and inertial interaction which relates to mass properties of the structure. In the pioneering works done by Jennings and Bielak [1], Veletsos and Meek [2], Veletsos and Nair[3], and Veletsos [4] improved a replacement oscillator, which has modified period and damping values according to soil-structure interaction effect for the single degree of freedom system (SDOF) by taking the foundation input motion (FIM) as free field motion (FFM) because of surface foundation situation. Although their approximation is reasonable only for surface foundations, Bielak [5], and Aviles and Perez-Rocha [6] analyzed embedded foundations under the FFM neglecting the effect of KI. KI is also neglected at American design codes [7-10]. On the other hand, in Japanese design code, KI is considered but rocking foundation input motion (RFIM) is not considered [11]. Nevertheless, according to Luco [12], using the horizontal and rocking foundation input motion (RFIM) instead of FFM is important for reliable results. Moreover, according to Morray [13], the peak values of the acceleration response spectra are underestimated if the effect of the RFIM is neglected. Therefore, the sensitivity of analyses on RFIM should be researched.

Moreover, according to Kawashima *et al.* [14], effect of rocking component of effective input motion increases with increasing

* Grad. Stud., Graduate School of Env. Studies, Nagoya University
名古屋大学大学院環境学研究科　大学院生
** Designated Prof., Disaster Mitigation Research Center, Nagoya Univ., Dr.Eng.
名古屋大学減災連携研究センター　特任教授・博士(工学)
*** Prof., Disaster Mitigation Research Center, Nagoya Univ., Dr.Eng.
名古屋大学減災連携研究センター　教授・工博

high frequency component of input motion according to results of large shaking table test study, and correlativity of horizontal and rocking component of effective input motion is low. Kawashima *et al.* [15] assert that stiffness of superstructure has an influence on rocking component of effective input motion and rocking component of effective input motion is more effective on short period structures according to 86 seismic events within the 14 years in Japan. On the other hand, in our study foundation input motion is used instead of effective foundation input motion that also includes effect of response of superstructure in the analyses.

All the aforementioned studies include only elastic soil-structure systems. However, as it is known, structures behave severely beyond the elastic region of the material during strong earthquakes. The early study about the response of elasto-plastic structure considering SSI is done by Veletsos and Vebric [16]. In their study, it is asserted that the effect of inelasticity of structure diminishes the relative stiffness of structure to the soil, therefore the effect of SSI decreases. According to Bielak [17], on the resonant frequency, structural deformations become large for an inelastic structure having a surface foundation. Lin and Miranda [18] research the effect of SSI on the maximum inelastic deformation of SDOF systems by taking the KI effect as the low-pass filter. Jarernprasert *et al.* [19] analyse the SDOF elasto-plastic structure embedded in elastic soil without the KI effect. Moreover, Mahsuli and Ghannad [20] assert that ductility demands for embedded foundations increase with increasing their embedment ratios, especially for the embedment ratios bigger than one due to the effect of RFIM. And in their study the lumped parameter model (LPM) given as Wolf [21] for embedded foundations is used as a soil model for the analyses. Although this model is very convenient to consider the nonlinearity of superstructures due to having frequency independent elements, it is built up for Poisson's ratio equals to 0.25 because of the lack of reliable data for other values of this parameter. However, as it is known, for soft soil conditions, where SSI effects can be seen more severely, Poisson's ratios are observed higher, up to 0.5. Moreover, in the aforementioned study, height of the SDOF structure is taken independently from the fixed base natural frequency which may represent unrealistic structural characteristics, and only records of active fault earthquakes are considered, so the results cannot be generalized to subduction zone related earthquakes.

In this study a new LPM is constructed depending on the impedances of embedded foundations having different embedment depth placed on the elastic half-space for the Poisson's ratio equals to 0.42 and shear wave velocity value equal to 100 and 200 m/s to represent the soft soil conditions. Poisson's ratio is selected as 0.42 as a case of soft soil condition and fixed for the analyses in this study. Moreover, it should be noted that this method is applicable for other Poisson's ratios. After that non-linear earthquake response analyses by using the proposed LPM model are carried out under active fault and subduction zone earthquake records considering with and without RFIM to get the effects of RFIM on the ductility demands of structures. Additionally, it can be said that the method of analysis is more reliable than the Mahsuli and Ghannad [20], because the created LPM is more reliable for soft soil conditions (Poisson's ratio equals to 0.42 instead of equal to 0.25) where SSI effect can be seen more severely and the parameters selected for the superstructure make easier to understand which kind of structures are affected from SSI intensively by taking predominant periods (between 0.2 and 3 seconds) of superstructure related to their aspect ratios and assuming the ductility capacities under the fixed based condition as 2, 4, and 6.

2. Analysis Model and Method

2.1 Analysis Flow

As it is known, determining the exact impedances and input motions for foundations requires rigorous mathematical techniques such as the finite element method. To manage this, Meek and Wolf [22] assert a simplified method by using double cone analysis to obtain the impedances and FIM of embedded foundations. Due to the simplicity, the lumped parameter method improved by Wolf [21] is used and the horizontal and rocking foundation input motions are calculated by double cone analysis [23].

The flowchart of the method can be seen in Figure 1. The analysis is applied in the two stages: first driving horizontal and rocking motions are calculated and then these forces are implemented to get the total motions of structure.

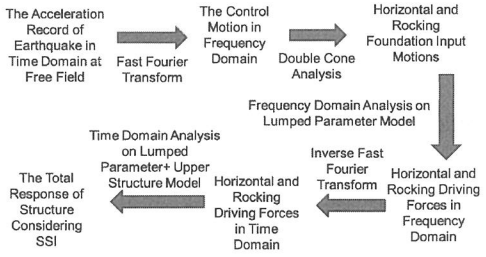

Fig. 1 Flowchart of the analysis method

2.2 Outline of New LPM

A LPM is a very efficient tool for time domain analysis of SSI, since it has spring, dashpot, and masses which are frequency independent, and also it is able to be analyzed under the well-known numerical methods, according to Saitoh [24]. In this study, a new LPM is improved by using the systematic procedure of Wolf [21] for the Poisson's ratio of soil equals to 0.42. In this method the exact values of dynamic stiffness, which are obtained by different techniques such as the TLM, are divided into the regular and singular part (the value of the impedance calculated by using dimensionless spring and dashpot values for infinite

frequency) as it is seen in Equation (1), Equation (2) and (3) respectively according to the rule of Wolf [21]. In these equations S is the dynamic stiffness, S_s is the singular part of the dynamic stiffness, S_r is the remaining regular part of the dynamic stiffness, K is the static stiffness, p and q are real coefficients of the polynomials, N is the degree of polynomial placed on the denominator, $k(a_0)$ and $c(a_0)$ are spring and dashpot coefficients of the dynamic stiffness, k and c are values of spring and dashpot coefficients of the dynamic stiffness at the infinite frequency, and a_0 is the dimensionless frequency that can be seen in Equation (4), where ω is the circular frequency, V_s is the shear wave velocity of the soil, and r is the radius of the foundation.

$$S(a_0)=K[k(a_0)+ia_0c(a_0)]=S_s(a_0)+S_r(a_0) \tag{1}$$

$$\frac{S_s(a_0)}{K}=k+ia_0c \tag{2}$$

$$\frac{S_r(a_0)}{K}\cong\frac{S_r(ia_0)}{K}=\frac{P(ia_0)}{KQ(ia_0)} =\frac{1-k+p_1ia_0+p_2(ia_0)^2+\ldots+p_{N-1}(ia_0)^{N-1}}{1+q_1ia_0+q_2(ia_0)^2+\ldots+q_N(ia_0)^N} \tag{3}$$

$$a_0=\frac{\omega r}{V_s} \tag{4}$$

Next, $2N+1$ real unknown $p_{1,\ldots,N+1}$ and $q_{1,\ldots,N}$ are determined by curve fitting technique on S_r by using the least square method to obtain a minimum ε^2 value as it is seen in Equation (5) where Q and P represent the polynomials placed on the numerator and denominator of Equation (3) respectively and $w(a_0)$ is the weight function.

$$\varepsilon^2=\sum_{j=1}^{J}w(a_{0j})\left|S_r(a_{0j})Q(ia_{0j})-P(ia_{0j})\right|^2 \tag{5}$$

After that, the regular part of the dynamic stiffness is written in the form of the partial fraction expansion at Equation (6) where s_ℓ are the roots of Q, A_ℓ are the residues at the poles.

$$\frac{S_r(ia_0)}{K}=\sum_{\ell=1}^{N}\frac{A_\ell}{ia_0-s_\ell} \tag{6}$$

Since the N is taken as 1 in this study, Equation (6) can be written in the form of Equation (7) for $N=1$.

$$\frac{S_r(ia_0)}{K}=\frac{A_1}{ia_0-s_1} \tag{7}$$

The dynamic stiffness of the foundation can be represented by a combination of the models seen in Figure 2 and Figure 3 physically. If we consider the dynamic stiffness of the model seen in Figure 2 and given in Equation (8), we can easily determine the A_1 and s_1 values to match the dynamic stiffness of the model to the regular part of the dynamic stiffness by using Equations (9)-(10).

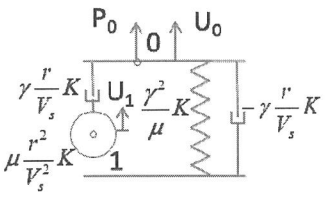

Fig. 2 The model selected to represent the regular part of the dynamic stiffness

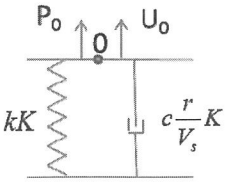

Fig. 3 The model selected to represent the singular part of the dynamic stiffness

$$\left(\frac{\frac{\gamma^3}{\mu^2}}{ia_0+\frac{\gamma}{\mu}}\right)U_0(a_0)=\frac{P_0(a_0)}{K} \tag{8}$$

$$\gamma=\frac{A}{s_1^2} \tag{9}$$

$$\mu=-\frac{A}{s_1^3} \tag{10}$$

And the singular part of the dynamic stiffness can be represented by the model seen in Figure 3. This systematic lumped parameter method rule is taken from Wolf [21].

The aforementioned technique is reliable when coupling is neglected. However, as it is known, horizontal and rocking degree of freedoms of embedded foundations interact with each other. To solve this issue, discrete impedance values represented by horizontal, rocking and coupling parts of the model are calculated as it is shown in Equations (11)-(13), where e is the embedment depth of the foundation, S_{hh}, S_{rr}, and S_{hr} are horizontal, rocking, coupling dynamic stiffness values of the rigid foundation respectively. S^m_{hh}, S^m_{rr}, and S^m_{hr} are dynamic stiffness values of horizontal, rocking, and coupling part of this model respectively. By using this discretization, the curve fitting technique can be applied to each part of the model separately.

The new model is shown in Figure 4. The main difference of this model from that introduced by Wolf [21] for embedded foundations is that this model has a fictitious mass not only for rocking part but also for coupling part due to the high frequency dependence of the coupling impedance.

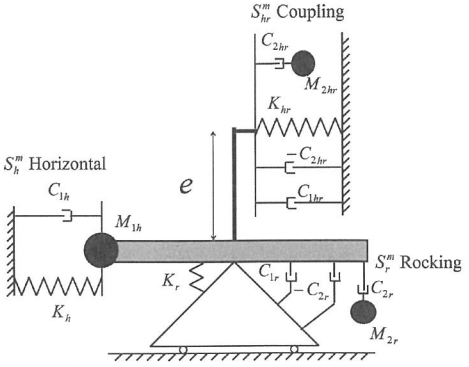

Fig. 4 A new LPM model produced in this study

$$S^m_{hr}(\omega)=\frac{S_{hr}(\omega)}{e} \tag{11}$$

$$S^m_{hh}(\omega)=S_{hh}(\omega)+\frac{S_{hr}(\omega)}{e} \tag{12}$$

$$S^m_{rr}(\omega)=S_{rr}(\omega)+eS_{hr}(\omega) \tag{13}$$

The dynamic stiffness of horizontal, rocking and coupling part of the model seen in Figure 4 are given in Equations (14)-(16) respectively.

$$S^m_{hh}(\omega)=\left(-\omega^2 M_{1h}+K_h+i\omega C_{1h}\right) \tag{14}$$

$$S^m_{rr}(\omega)=-\omega^2 M_{1r}+K_r+i\omega C_{1r}-i\omega C_{2r}\frac{i\omega C_{2r}}{-\omega^2 M_{2r}+i\omega C_{2r}} \tag{15}$$

$$S^m_{hr}(\omega)=-\omega^2 M_{1hr}+K_{hr}+i\omega C_{1hr}-i\omega C_{2hr}\frac{i\omega C_{2hr}}{-\omega^2 M_{2hr}+i\omega C_{2hr}} \tag{16}$$

Equations of the parameters are given in Equations (17)-(27) where C_1, C_2, M_1, M_2 and K are lumped values for damping, mass and spring having subindices h for horizontal, r for rocking, hr for coupling component of the model. $K_{correct}$ is the correcting coefficient used for better fit to exact impedances. K^m_{hh}, K^m_{rr}, K^m_{hr} represents the static stiffness of horizontal, rocking and coupling part of the model respectively. γ_1, γ_2, μ_1, and μ_2 are dimensionless values.

$$C_{1h}=\gamma_{1h}\frac{r}{V_s}K^m_{hh} \tag{17}$$

$$C_{1r}=\gamma_{1r}\frac{r}{V_s}K^m_{rr} \tag{18}$$

$$C_{1hr}=\gamma_{1hr}\frac{r}{V_s}K^m_{hr} \tag{19}$$

$$C_{2r}=\gamma_{2r}\frac{r}{V_s}K^m_{rr} \tag{20}$$

$$C_{2hr}=\gamma_{2hr}\frac{r}{V_s}K^m_{hr} \tag{21}$$

$$M_{1h}=\mu_{1h}\frac{r^2}{V_s^2}K^m_{hh} \tag{22}$$

$$M_{2r}=\mu_{2r}\frac{r^2}{V_s^2}K^m_{rr} \tag{23}$$

$$M_{2hr}=\mu_{2hr}\frac{r^2}{V_s^2}K^m_{hr} \tag{24}$$

$$K_h=Kh_{correct}K^m_{hh} \tag{25}$$

$$K_r=Kr_{correct}K^m_{rr} \tag{26}$$

$$K_{hr}=Khr_{correct}K^m_{hr} \tag{27}$$

The static stiffness of horizontal, rocking and coupling part of the model are given in Equations (28)-(30) where G is the shear modulus of the soil, r is the radius of the foundation, e is the embedment depth of the foundation.

$$K^m_{hh}=\frac{16Gr}{3(2-\nu)}\left(1+\frac{e}{r}\right) \tag{28}$$

$$K^m_{rr}=\frac{8Gr^3}{3(1-\nu)}\left(1+2.3\frac{e}{r}+0.58\left(\frac{e}{r}\right)^3\right)-\frac{8Gr^3}{3(2-\nu)}\left(\frac{e^2}{r^2}+\frac{e^3}{r^3}\right) \tag{29}$$

$$K^m_{hr}=\frac{8Gr}{3(2-\nu)}\left(1+\frac{e}{r}\right) \tag{30}$$

Finally, the dimensionless coefficients of the model for different embedment ratios (e/r) are given in Table 1. As it is seen in the table, there is no coupling part for surface foundation (e/r=0), and coupling part for the embedment ratio which equals to 0.25 has only one spring and dashpot. It means that the coupling impedance does not so depend on excitation frequency for low embedment ratios.

Table 1 The dimensionless parameters of LPM for Poisson's ratio equals to 0.42

	e/r=0.00	e/r=0.25	e/r=0.50	e/r=1.00	e/r=1.50	e/r=2.00
$Kh_{correct}$	1.000	1.109	1.102	1.050	0.995	0.948
$Kr_{correct}$	1.000	0.886	0.858	0.895	0.898	0.878
$Khr_{correct}$	1.000	0.605	0.936	1.056	1.069	1.057
γ_{1h}	0.608	0.552	0.798	1.064	1.241	1.416
γ_{1r}	0.460	0.450	0.421	0.268	0.019	-0.355
γ_{1hr}	-	1.694	1.224	1.627	1.930	2.168
γ_{2r}	0.413	0.436	0.406	0.381	0.440	0.512
γ_{2hr}	-	-	0.082	0.416	0.514	0.575
μ_{1h}	-	-	0.029	0.050	0.082	0.103
μ_{2r}	0.178	0.190	0.165	0.145	0.194	0.263
μ_{2hr}	-	-	0.007	0.173	0.264	0.330

2.3 Determining the Parameters of LPM

2.3.1 Comparing the Impedances obtained by TLM and LPM

TLM is a semi-analytical method on which dynamic response of foundations on layered soils can be computed by dividing the soils into thin layers horizontally, according to Park [25]. This method is improved by Tajimi [26], Waas [27] and Kausel [28] during the same year. In this study, the impedances obtained by TLM analyses are assumed as exact values, and a new LPM is built up by using the curve fitting technique improved by Wolf [21] on these impedances.

The soil and foundation model can be seen in Figure 5. To calculate the homogeneous elastic half-space by TLM, the soil is divided into the thin layers with increasing thickness from bottom to top. Moreover, to represent unbounded soil, paraxial boundary is applied to the bottom of model. Moreover, a circular rigid foundation placed on this half-space is also divided into the elements to calculate impedances by using finite element method (FEM), as it is seen in Figure 5 (Wen *et al.* [29]).

The comparison of the spring and dashpot coefficients calculated by LPM and TLM can be seen in Figures 6-11, for each e/r (=0.5, 1.0, 2.0).

As it is seen in these figures, horizontal spring and dashpot

coefficients fit with the exact values nearly for whole dimensionless frequency range, but approximation for rocking spring and dashpot coefficients seems not so good, within the error ratio equals to 20%. Moreover, coupling spring coefficients fit with exact values better for the dimensionless frequency smaller than 1.5.

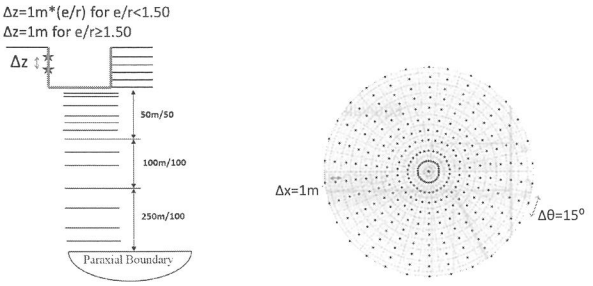

Fig. 5 Soil model by TLM and model of the foundation by FEM

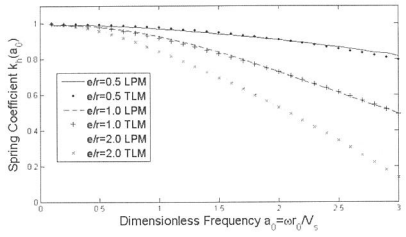

Fig. 6 Spring coefficients for horizontal component (k_h) for the embedded foundations

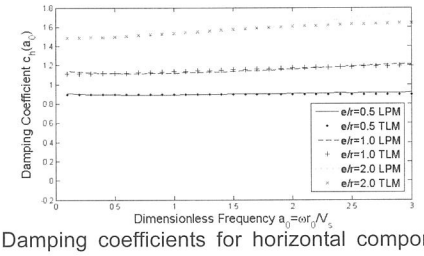

Fig. 7 Damping coefficients for horizontal component (c_h) for the embedded foundations

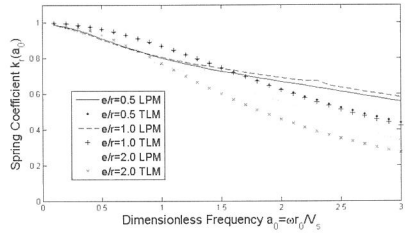

Fig. 8 Spring coefficients for rocking component (k_r) for the embedded foundations

2.3.2 Verifying LPM

To verify the improved LPM, the transfer functions obtained by classical frequency domain analysis (FDA) and LPM are compared in the Figure 12 where the shear wave velocity of soil (V_s) is 100 m/s and natural period of superstructure (T_{fix}) is 1 and 0.5 sec respectively. As it is seen in these figures, transfer functions by LPM are good agreement with those by FDA. According to results, it can be said that this approximation is almost adequate.

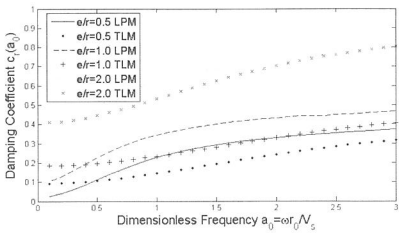

Fig. 9 Damping coefficients for rocking component (c_r) for the embedded foundations

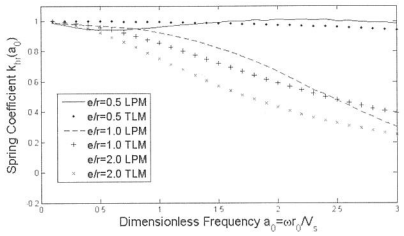

Fig. 10 Spring coefficients for coupling component (k_{hr}) for the embedded foundations

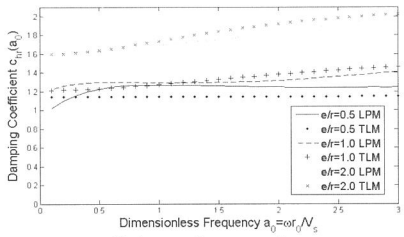

Fig. 11 Damping coefficients for coupling component (c_{hr}) for the embedded foundations

2.4 Determining Driving Forces

As it is known, driving forces are the forces required to make foundation motionless under the FIM. To get them, LPM should be analyzed in the frequency domain.

Driving forces are given in Equation (31), where P_g is horizontal driving force, M_g is rocking driving force, u_g is horizontal foundation input motion (HFIM) and θ_g is RFIM.

$$\begin{bmatrix} S_{hh}^m(\omega)+S_{hr}^m(\omega) & eS_{hr}^m(\omega) \\ eS_{hr}^m(\omega) & S_{rr}^m(\omega) \end{bmatrix} \begin{Bmatrix} u_g(\omega) \\ \theta_g(\omega) \end{Bmatrix} = \begin{Bmatrix} P_g(\omega) \\ M_g(\omega) \end{Bmatrix} \tag{31}$$

If u_g and θ_g are taken as given above, this situation equals to "with RFIM". If θ_g is taken as zero for same u_g, this situation equals to "without RFIM". If u_g is taken as the free field motion (FFM) and θ_g is taken as zero, this situation equals to "without

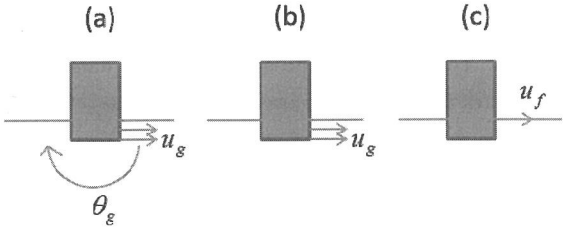

Fig. 12 Analysis conditions (a) With RFIM (b) Without RFIM (c) Without KI

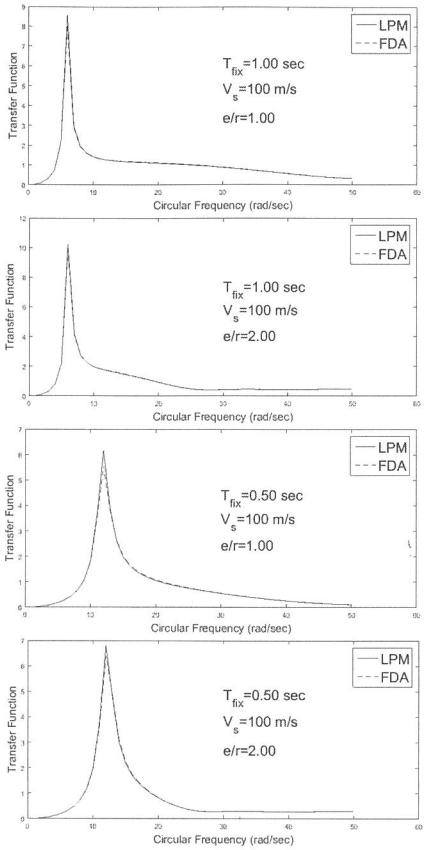

Fig. 13 Transfer functions obtained by FDA and LPM

KI" in this study. These situations are given in Figure 13 where u_f is FFM graphically. The differences of the effect of these situations on the nonlinear behavior of superstructure are researched.

3. Analysis Conditions

3.1. Model of SDOF structure

To cover the existing residential buildings, a simple approximation is applied to determine the parameters of the structure as it is seen in Figure 14, where T_{fix} is natural period of the SDOF system under the fixed base situation, N is the number of stories, M_{floor} is the mass of each floor of the structure, b_{floor} is the thickness of the floor, b_{found} is the thickness of the foundation, ΔH is the story height, H is the total height of the structure and H_{eff} is the effective height of the structure. Mass ratio of the foundation to the structure is taken as 0.82 and analyses are done for the embedment ratios of foundations (e/r) which equal to 0, 0.5, 1.0, and 2.0. Foundations are considered as infinitely rigid. The initial stiffness proportional damping is applied. Newmark-Beta Method is used and ß is set as 0.25.

For simplicity, the inelasticity of structures is represented by elasto-plastic models with zero hardening after yielding as it seen in Figure 15. The yield strength is assumed so that the maximum ductility factor may equal to μ_{fix} as a given value under the fixed base model.

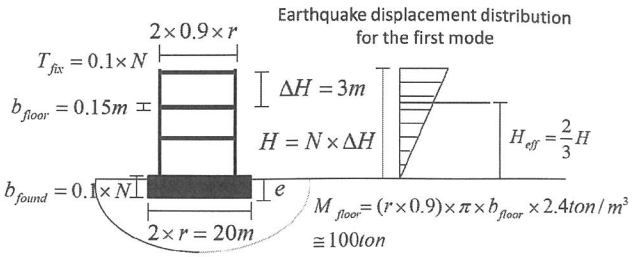

Fig. 14 Analysis model for superstructures

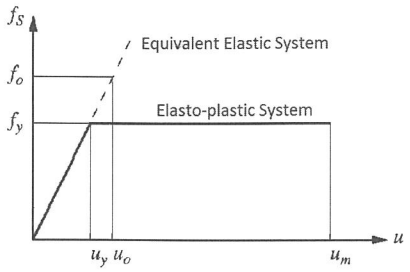

Fig. 15 Elasto-plastic model of superstructures used in this study. f_0, f_y, u_0, u_y and u_m are the elastic demand of strength, yield strength, elastic displacement demand, yield displacement and ultimate displacement of the system, respectively

3.2. Soil Parameters

The soil is idealized as homogeneous elastic half-space having no material damping. Mass density of soil (ρ) is considered as 1.8 ton/m^3, and shear wave velocity of soil (V_s) is selected as 100 and 200 m/s. To represent the soft soil condition, Poisson's ratio of soil (ν) is taken as 0.42.

3.3. Selected Earthquake Records

The 1995 Hyogoken-Nanbu (Kobe Earthquake) TAK000 component of Takatori Station Record is chosen as an input motion. According to Mylonakis *et al.* [30], one of the main reasons of collapsing of 18 piers of Hanshin Expressway during the 1995 Hyogoken-Nanbu Earthquake, where it is placed near to Takatori Station, is soil-structure interaction. Moreover, to see the effect of subduction zone earthquake record which has similar amplitude level, more peaks on acceleration spectra and longer duration of the record than Kobe Earthquake record on the response of superstructure, the 2011 off the Pacific Coast of Tohoku Earthquake (Tohoku Earthquake) EW component of MYG006 Station (K-NET Furukawa) is also used for analyses. The acceleration time histories and acceleration response spectra (h=5%) of the records are given in Figures 16-18 respectively.

4 Effect of RFIM on the Response of Superstructure

4.1. Analysis Results for Kobe Earthquake Record

In this section, non-linear seismic response analyses are conducted using the proposed analytical model to analyze the effect of the rocking foundation input motion (RFIM) on the responses of superstructures.

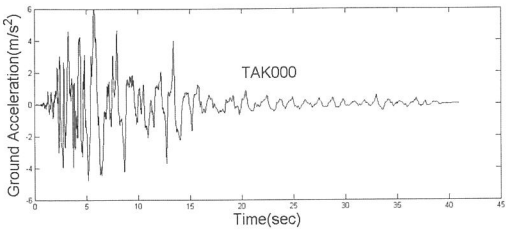

Fig. 16 Acceleration time history of Kobe Earthquake TAK000 component at Takatori Station

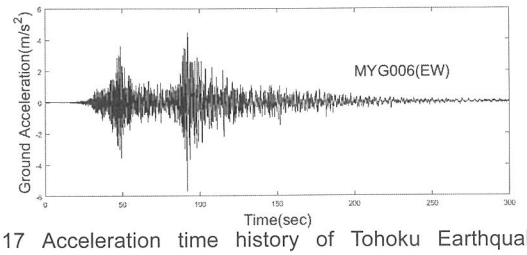

Fig. 17 Acceleration time history of Tohoku Earthquake EW component at MYG006 Station

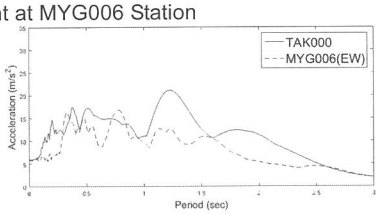

Fig. 18 Acceleration response spectra of TAK000, and MYG006 (EW) records (h=5%)

Specifically, time history non-linear response analyses are carried out under some input motions considering the kinematic interaction by using the proposed analysis model. The effect of the RFIM on the non-linear response of the superstructure is studied by comparing the maximum ductility factor μ_{max} with μ_{fix} in the case of the different embedment depth of foundation.

The results obtained by using Kobe Earthquake record are shown in Figs. 19 – 22 where x axis is the natural period of the superstructure that represents number of stories of the superstructure from 2 to 30 stories. All graphs show the ratio of maximum response ductility factor μ_{max} to μ_{fix}. Figs. 19 to 21 show results in the case of the shear wave velocity Vs = 100m/s of surface ground and μ_{fix} = 2, 4, and 6. Figure 22 shows the results in the case of the shear wave velocity Vs = 200m/s of surface ground and μ_{fix} = 2. In each figure, (a) with RFIM, (b) without RFIM, (c) without KI are shown.

First, the difference of the results that under the conditions (a) with RFIM and (c) without KI are explained. As shown in Figs. 19 to 21 (a) and (c), it is found that responses with RFIM are almost equal to those without KI for every μ_{fix} of middle rise buildings, but responses of low rise buildings with short natural period (natural period less than 0.5 sec) for (a) are smaller than (c) because of low-pass filter effect of KI. Therefore, it can be said that safer design is obtained for low rise buildings by neglecting KI.

Next, the difference of the results that under the conditions (a) with RFIM and (b) without RFIM are explained. It is clear that the responses of (b) are smaller than that of (a). In particular, as the μ_{fix} becomes larger and embedment depth becomes deeper, the difference between μ_{fix} and μ_{max} becomes more remarkable. It means that earthquake responses considering only horizontal kinematic interaction are underestimated.

Next, effect of RFIM on the buildings having long natural period is explained. When μ_{fix} is small, the responses of buildings with natural periods more than 2 seconds except for the e/r = 2 under considering RFIM are smaller than those of the fixed-base model. It is estimated that the input ground motion is reduced because the slender building with spread foundation on the soft ground is assumed and the rocking spring of the soil is relatively small and the natural period of the coupled system becomes long. However, if the embedment is deep (e/r = 2.0) considering RFIM, it is seen that the response is increasing because of the small rocking stiffness. In addition, when μ_{fix} is large, building responses of (a) are larger than those of the fixed base model in some case of the natural period of buildings, even if the embedment is shallow.

Finally, importance of RFIM on the nonlinear response of buildings is evaluated generally. It is notable that the maximum ductility factor of the e/r = 2.0 in Fig. 20 (a) are 1.5 times larger than that both of the fixed base model and (c) by means of the RFIM. Therefore, it can be said that unreasonable design is obtained for such conditions by neglecting KI or SSI. It suggests the possibility that the rocking input motion is a major impact in the near to the ultimate state situation of the building. However these results only valid for mat foundations, for pile foundations different study should be applied.

Fluctuation of ductility factors with changing natural frequency values is seen in these figures. Since, it is noticed that the global tendency of results may depend on the relationship between the spectral characteristics of the input ground motion and the equivalent natural period of the superstructure under the plastic deformation in this study. The aforementioned results are explained schematically at Table 2.

On the other hand, if the shear wave velocity of the surface layers is as large as Vs = 200m/s, as shown in Figure 22, the variation due to the difference in the embedment depth is less in any natural period, and that it is found the response exhibits almost the same response as the fixed base model in the case of (a) and (c).

Maximum response ductility factor ratio of (a): with RFIM to (c):without KI is compared with each μ_{fix} in Figure 23 where x-axis is same as Figs. 19 to 21. When the ratio is larger than 1, it means that the response ductility factor is increased by taking into account RFIM. From this figure, it is found that the response is underestimated in the case of the deep embedment

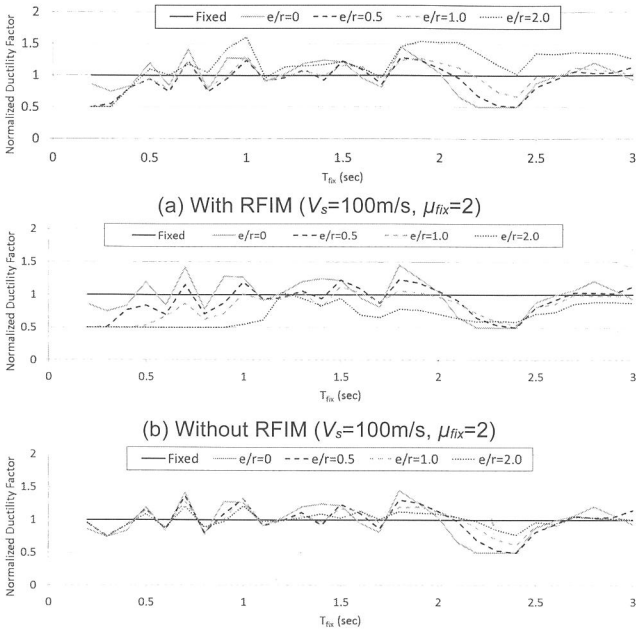

(a) With RFIM (V_s=100m/s, μ_{fix}=2)

(b) Without RFIM (V_s=100m/s, μ_{fix}=2)

(c) Without KI (V_s=100m/s, μ_{fix}=2)

Fig. 19 Ductility factors for Kobe Earthquake TAK000 component at Takatori Station with and without RFIM, and without KI (h=0.05, r=10m, $H_{eff}/r=2T_{fix}$, ρ=1.8t/m^3, V_s=100 m/s, v=0.42, $m=N$*100t, m_f/m=0.82, μ_{fix}=2)

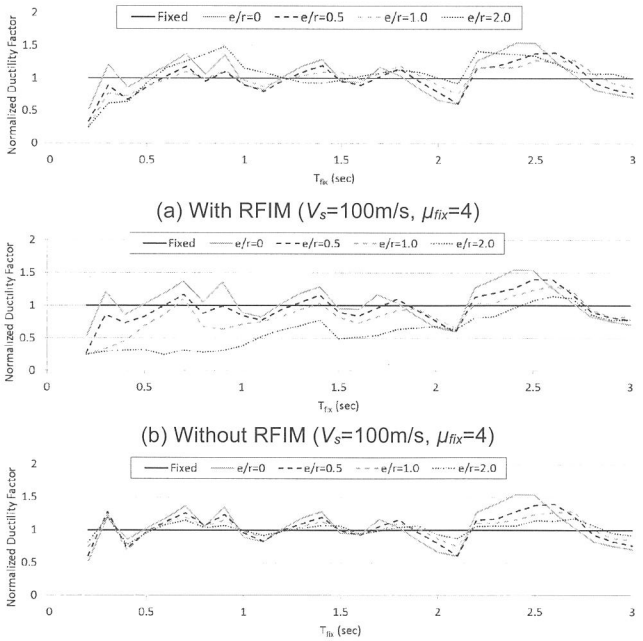

(a) With RFIM (V_s=100m/s, μ_{fix}=4)

(b) Without RFIM (V_s=100m/s, μ_{fix}=4)

(c) Without KI (V_s=100m/s, μ_{fix}=4)

Fig. 20 Ductility factors for Kobe Earthquake TAK000 component at Takatori Station with and without RFIM, and without KI (h=0.05, r=10m, $H_{eff}/r=2T_{fix}$, ρ=1.8t/m^3, V_s=100m/s, v=0.42, $m=N$*100t, m_f/m=0.82, μ_{fix}=4)

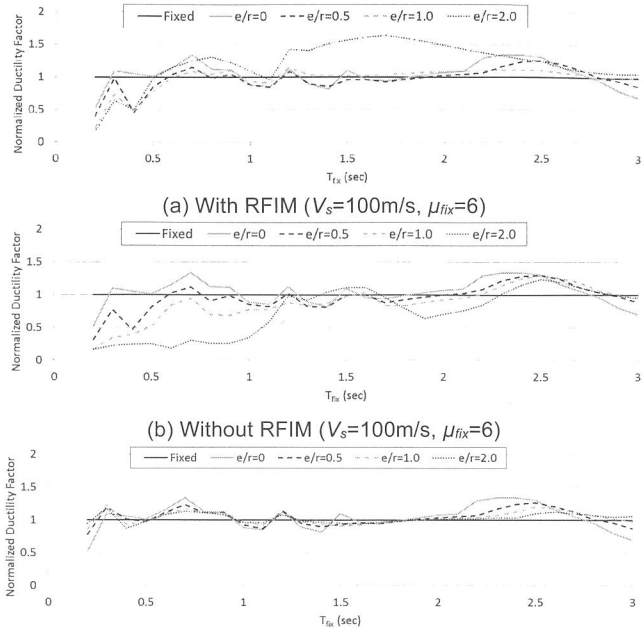

(a) With RFIM (V_s=100m/s, μ_{fix}=6)

(b) Without RFIM (V_s=100m/s, μ_{fix}=6)

(c) Without KI (V_s=100m/s, μ_{fix}=6)

Fig. 21 Ductility factors for Kobe Earthquake TAK000 component at Takatori Station with and without RFIM, and without KI (h=0.05, r=10m, $H_{eff}/r=2T_{fix}$, ρ=1.8t/m^3, V_s=100m/s, v=0.42, $m=N$*100t, m_f/m=0.82, μ_{fix}=6)

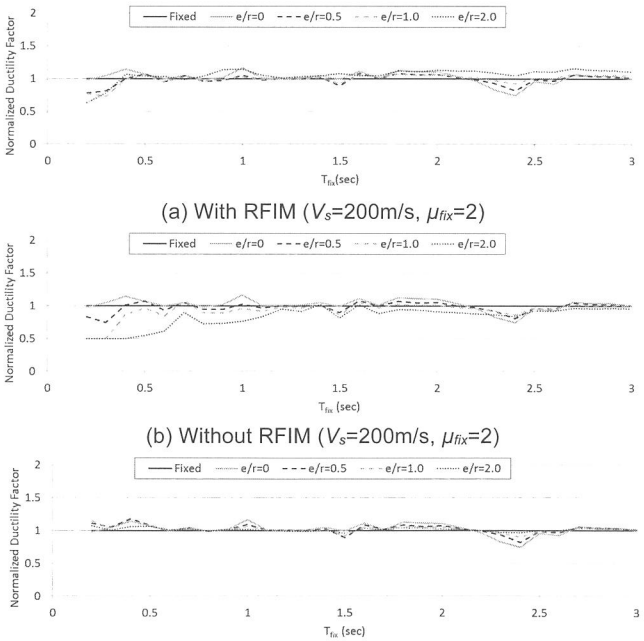

(a) With RFIM (V_s=200m/s, μ_{fix}=2)

(b) Without RFIM (V_s=200m/s, μ_{fix}=2)

(c) Without KI (V_s=200m/s, μ_{fix}=2)

Fig. 22 Ductility factors for Kobe Earthquake TAK000 component at Takatori Station with and without RFIM, and without KI (h=0.05, r=10m, $H_{eff}/r=2T_{fix}$, ρ=1.8t/m^3, V_s=200m/s, v=0.42, $m=N$*100t, m_f/m=0.82, μ_{fix}=2)

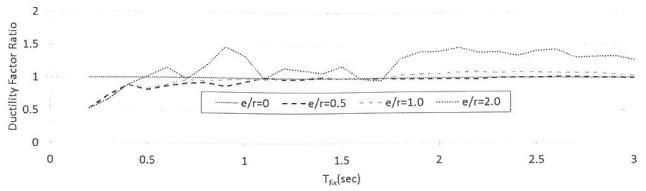

(a) μ_{fix}=2

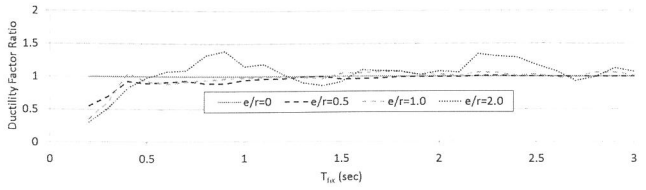

(b) μ_{fix}=4

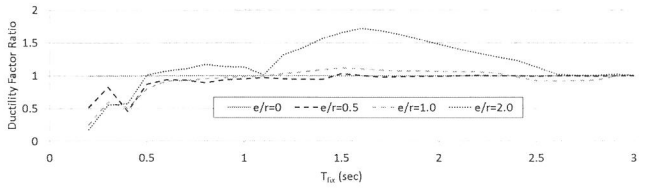

(c) μ_{fix}=6

Fig. 23 Ductility factor Ratios for Kobe Earthquake TAK000 component at Takatori Station with RFIM to without KI (h=0.05, r=10m, $H_{eff}/r=2T_{fix}$, ρ=1.8t/m^3, V_s=100m/s, v=0.42, $m=N$*100t, m_f/m=0.82)

Table 2 Schematic representation of the discussion of the results of the analyses (for V_s=100m/s)

(a) (c)	For middle rise buildings ⇒ Responses for (a) and (c) are almost equal For low rise buildings ⇒ Responses for (a) < (c)
(a) (b)	Responses for (b) smaller than (a) For ↑μ_{fix} and ↑ e/r ⇒ Difference between μ_{fix} and μ_{max} ↑
T_{fix} → long (a) μ_{fix}=6	For e is shallow(in the case of the study e/r≤1) ⇒ Responses for (a)≈ Fixed based model For e is deep (in the case of the study e/r=2) ⇒ Responses for (a)> Fixed based model Due to small rocking stiffness

foundation in 0.5 seconds or more of the building natural period if RFIM is neglected.

4.2 Analysis Results for Tohoku Earthquake Record

The results of Vs = 100m/s and μ_{fix} = 6 are shown in Figure 24. In this case, the observation records at K-NET Furukawa (MYG006) of the main shock (EW component) in the 2011 Tohoku region Pacific Ocean Earthquake is applied as an input ground motion. It is found that μ_{max} fluctuates according to the spectral characteristic of the input ground motion in the long period domain. In Figure 25, maximum ductility factor ratio of (a): with RFIM to (c): without KI is compared to the case of μ_{fix} =6. The same tendency as that of the Kobe Earthquake is shown. From these results, it is concluded that inelastic building

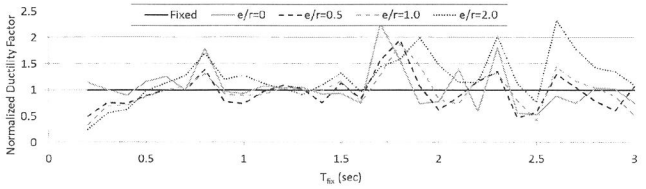

(a) With RFIM (V_s=100m/s, μ_{fix}=6)

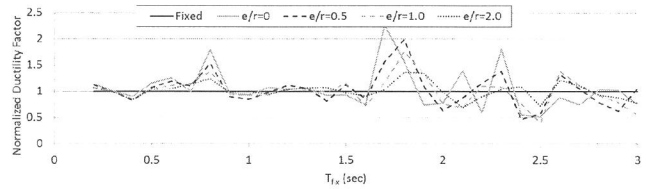

(b) Without KI (V_s=100m/s, μ_{fix}=6)

Fig. 24 Ductility factors for Tohoku Earthquake EW component at MYG006 with RFIM, and without KI (h=0.05, r=10m, $H_{eff}/r=2T_{fix}$, ρ=1.8t/m^3, Vs=100 m/s, v=0.42, m=N*100t, mf/m=0.82, μ_{fix}=6)

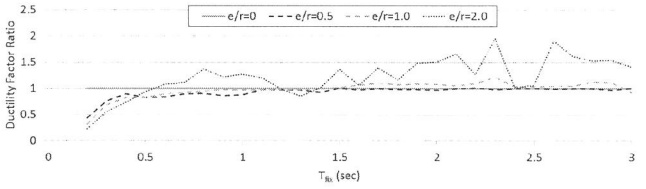

Fig. 25 Ductility factor Ratios for Tohoku Earthquake EW component at MYG006 with RFIM to without KI (h=0.05, r=10m, $H_{eff}/r=2T_{fix}$, ρ=1.8t/m^3, V_s=100m/s, v=0.42, $m=N$*100t, m_f/m=0.82, μ_{fix}=6)

responses are not dependent strongly on duration of input ground motions in this study.

5. Conclusions

In this study a new LPM is constructed depends on the impedances of embedded foundations having different embedment depth placed on the elastic half-space for the Poisson's ratio equals to 0.42 and shear wave velocity value equal to 100 and 200 m/s to represent the soft soil conditions. Verification is done by using the horizontal, rocking, coupling impedances of the model and the response of superstructure. According to comparison, it can be said that approximation is almost adequate.

Then nonlinear response analyses are carried out by an SDOF elasto-plastic structure, having fixed ductility capacity values as 2, 4, 6, and predominant periods from 0.2 to 3 seconds, and the proposed LPM model under active fault and subduction zone earthquake records considering with and without RFIM to get effects of RFIM on the ductility demands of superstructures. Earthquake records both of Takatori Station record in the 1995 Hyogoken-Nanbu Earthquake (Kobe Earthquake) and the 2011 off the Pacific Coast of Tohoku Earthquake (Tohoku Earthquake) EW component of MYG006 Station are used for these analyses. The results of analyses are shown as follows;

a. By increasing ductility factor values, the effect of

RFIM becomes more important, especially for high-rise buildings having embedment ratios bigger than 1. The reason of this phenomena is considered that the equivalent elastic stiffness of superstructure becomes softer for increasing values of ductility capacity, therefore inertial interaction becomes less important and the additional force coming from the rocking motion becomes more important in the response of superstructure.

b. For V_s=200 m/s, the effect of RFIM is more limited than V_s=100m/s, because the amplitude of RFIM decreases.

c. As a suggestion for design, RFIM should be considered for the collapse limiting design especially for the high rise building having embedment ratios bigger than 1 in this case. Even the design by neglecting the kinematic interaction, underestimates the effect of earthquakes in some critical situations.

However, it should be noted that these results are obtained for restricted parameters. For more reliable results, considered parameters in the analyses should be increased.

As future works, same research can be conducted for layered soil condition and including geometric and material soil nonlinearity to obtain more general results. Moreover, different kind of foundation types such as pile foundation case and the effect of structure-soil-structure interaction (SSSI) can be considered in the analyses.

Acknowledgement

Professor Jun Tobita gives us good advices and the program coded by Doctor Xuezhang Wen is used to calculate impedances in this study. Moreover, refers give us useful comments. The authors gratefully acknowledge contribution of them.

REFERENCES

1)Jennings PC, Bielak J.: Dynamics of buildings–soil interaction. *Bulletin of Seismological Society of America* 63(1), pp.9–48, 1973.

2)Veletsos AS, Meek JW.: Dynamic behavior of building–foundation system. *Earthquake Engineering and Structural Dynamics* 3(2):pp.121–138, 1974.

3)Veletsos AS, Nair VVD.: Seismic interaction of structures on hysteretic foundations. *Journal of the Structural Division (ASCE)* 101(1), pp.109–129, 1975.

4)Veletsos AS.: Dynamics of structure–foundation systems. *In Structural and Geotechnical Mechanics, Hall WJ (ed.),* A Volume Honoring N.M. Newmark. Prentice-Hall: Englewood Cliffs, NJ, pp.333–361, 1977.

5)Bielak J.: Dynamic behavior of structures with embedded foundations. *Earthquake Engineering and Structural Dynamics* 3(3), pp.259–274, 1975.

6)Avilés J, Pérez-Rocha LE.: Soil-structure interaction in yielding systems. *Earthquake Engineering and Structural Dynamics* 32(11), pp.1749–1771, 2003.

7)Applied Technology Council. Tentative provisions for the development of seismic regulations for buildings. ATC-3-06, California, 1978.

8)Building Seismic Safety Council (BSSC). NEHRP Recommended Provisions for Seismic Regulations for New Buildings and Other Structures. Federal Emergency Management Agency, Washington, DC, 2000.

9)FEMA 440. Improvement of nonlinear static seismic analysis procedures. Report No. FEMA 440, Federal Emergency Management Agency, prepared by Applied Technology Council, 2005.

10)Building Seismic Safety Council (BSSC), 2009: NEHRP Recommended Provisions for Seismic Regulations for New Buildings and Other Structures. Federal Emergency Management Agency, Washington, DC.

11) Structure related technical standard manual for buildings (2007 year edition) (in Japanese), Structure related technical standard manual for buildings edit committee, 2008.6

12)Luco JE, Wong HL, Trifunac MD.: A note on the dynamic response of rigid embedded foundations. *Earthquake Engineering and Structural Dynamics* 4(2), pp.119–127, 1975.

13)Morray JP.: Kinematic interaction problem of embedded circular foundations. M.Sc. Thesis, Department of Civil Engineering, Massachusetts Institute of Technology, 1975.

14)Kawashima M, Iguchi M, Minowa C.: Extraction of effective input motions to structures based on earthquake observations and a measure for the input motions. *J. Struct. Constr. Eng., AIJ,* No.615, pp.85-92, 2007.5.

15) Kawashima M, Iguchi M, Kashima T.: Variation of effective input motions to superstructure based on long term earthquake observation. *15 WCEE, Lizboa, Portugal,* 2012.

16)Veletsos AS, Verbic B.: Dynamics of elastic and yielding structure–foundation systems. *Proceedings of Fifth World Conference on Earthquake Engineering, Rome, Italy*, pp.2610–2613, 1973.

17)Bielak J.: Dynamic response of non-linear building–foundation systems. *Earthquake Engineering and Structural Dynamics* 6(1), pp.17–30, 1978.

18)Lin YY, Miranda E.: Kinematic soil–structure interaction effects on maximum inelastic displacement demands of SDOF systems. *Bulletin of Earthquake Engineering* 6(2), pp.241–259, 2008.

19)Jarernprasert, Sittipong, Enrique Bazan-Zurita, Bielak J.: Seismic soil-structure interaction response of inelastic structures. *Soil Dynamics and Earthquake Engineering* 47, pp.132-143, 2013.

20)Mahsuli M, Ghannad MA.: The effect of foundation embedment on inelastic response of structures. *Earthquake Engineering & Structural Dynamics* 38.4, pp.423-437, 2009.

21)Wolf JP.: Foundation vibration analysis using simple physical models. *Pearson Education*, 1994.

22)Meek JW, Wolf JP.: Cone models for embedded foundation. *Journal of geotechnical engineering* 120.1, pp.60-80, 1994.

23)Wolf JP, Deeks AJ.: Foundation vibration analysis: A strength of materials approach. Butterworth-Heinemann, 2004.

24)Saitoh, Masato.: Application of a Highly Reduced One-Dimensional Spring-Dashpot System to Inelastic SSI Systems Subjected to Earthquake Ground Motions, Advances in Geotechnical Earthquake Engineering - Soil Liquefaction and Seismic Safety of Dams and Monuments, Prof. Abbas Moustafa (Ed.), Chapter 14, 2012.

25)Park, J.: Wave motion in finite and infinite media using the thin-layer method. Diss. Massachusetts Institute of Technology, 2002.

26)Tajimi, H.: A Contribution to Theoretical Prediction of Dynamic Stiffness of Surface Foundation, *The 7th World Conference on Earthquake Engineering* Vol. 5, pp. 105-112, 1980.

27)Waas, G.: Dynamisch Belastete Fundamente auf Geschichtetem Baugrund, *VDI-Berichte* Nr. 381, pp. 185-189, 1980

28)Kausel, E.: An Explicit Solution for the Green Function for Dynamic Loads in Layered Media, Research Report R81-13, Department of Civil Engrg, M. I. T., Cambridge, Massachusetts, 1981

29)Wen, H.: An Analytical Study on Effects of Foundation Type, Foundation Shape and Adjacent Building on Dynamic Soil Structure Interaction. Diss. Nagoya University, 2006. (In Japanese)

30) Mylonakis, George, et al.: The role of soil in the collapse of 18 piers of Hanshin Expressway in the Kobe earthquake. *Earthquake Engineering & Structural Dynamics* 35(5), pp.547-575, 2006.

和文要約

1. はじめに

本論では、一般建物の耐震設計においてほとんど考慮されていない、根入れを有する基礎に作用する回転入力動が上部建物の非線形応答に与える影響について、新たな質点系モデルによる分析を行う。検討では、建物高さと根入れ深さ、及び入力地震動を主な検討パラメータとする。解析には、地盤ばねを有する2質点系モデルを用いている。地盤ばねは、振動数依存性を考慮できる Wolf[21]の手法を、ポアソン比が大きい軟弱な地盤に適用できるように拡張した。

2. 解析モデルと方法

2.1 解析フロー

応答計算においては、最初に、理論的に算定された基礎入力動から水平、及び回転方向のドライビングフォースを計算し、次に、これらのドライビングフォースを質点系の建物モデルに入力し、時刻歴非線形地震応答解析を実施する。

2.2 解析で用いる質点系モデルの概要

本論では、地盤ばねを有する質点系モデルを用いる。上部建物は、等価な1質点系に置換し、これに基礎（剛）を加えた2質点系とする。また、地盤ばねは、半無限一様地盤を対象とし、振動数依存型の水平、回転、水平—回転連成ばねを設定する。

2.3 質点系モデルにおける各種パラメータの設定

2.3.1 地盤ばねの設定方法と妥当性の検討

振動数依存型の地盤ばねは、付加質量やダッシュポット等で構成しており、各定数は、カーブフィッテング法により、精算解としての薄層要素法[29]による解析解に適合するように推定した。そして、水平インピーダンス、及び約1.5Hz以下における水平—回転連成インピーダンスは概ね対応した結果が得られた。ただし、回転インピーダンスは、他に比較して若干精度が低めに推定された。

2.3.2 質点系モデルの妥当性検証

次に、上記パラメータを用いた質点系モデルの妥当性について、建物応答の観点から検証した。検証では、地表に対する建物頂部の伝達関数を薄層要素法による解析結果と比較した。地盤のせん断波速度は Vs=100m/s、上部建物は5階建て（基礎固定時の一次固有周期を0.5秒）と10階建て（基礎固定時の一次固有周期を1秒）とし、さらに建物基礎の等価半径 r と根入れ深さ e の比 e/r として、0.0、0.5、0.25、1.0、1.5、2.0の6ケースを設定した。限られた範囲ではあるが、本モデルによる上部建物応答評価の妥当性を確認した。

2.4 ドライビングフォースの算定

本論では、ドライビングフォースとして、水平入力動と回転入力動の両方を考慮する場合、水平入力動だけを考慮する場合、地表面における水平入力動、すなわち、基礎固定と仮定した場合の3ケースを想定し、それらの違いが上部構造の地震時非線形挙動に与える影響について検討した。

3. 解析の諸条件

3.1 質点系モデルにおける上部建物の解析諸元

上部建物は、上述のように、等価な1質点系に置換する。検討では、階数と根入れ深さ、及び最大耐力をパラメータとしている。階数 N は2階～30階建てとし、基礎固定時の固有周期 T_{fix} を $0.1N$ として算定した。建築面積は、等価な半径 r として r=10m とし、根入れ深さ e は、半径 r との比 e/r として、0.0,0.5,1.0,2.0の4ケースを想定した。上部建物の復元力特性には、完全弾塑性モデルを用い、最大耐力は、基礎固定時の最大応答塑性率が指定された値 u_{fix} となるように設定した。ここでは、u_{fix} として、2,4,6の3ケースを想定した。なお、地盤ばねについては、線形としている。地震応答解析には Newmark-β法（β=0.25）用いた。

3.2 地盤の解析諸元

地盤は、半無限一様地盤で、せん断波速度が100m/s,200m/sの2ケースを想定し、地盤の固さの違いが回転入力動を伴う地震時建物応答に与える影響について分析する。

3.3 解析に用いた地震観測記録

入力地震動には、活断層の地震として、1995年兵庫県南部地震の葺合での観測記録を、海溝型地震として、2011年東北地方太平洋沖地震のK-NET古川（MYG006）のEW方向の観測記録を用いた。

4. 回転入力動が建物応答に与える影響

4.1 1995年兵庫県南部地震の観測記録に対する分析結果

ここでは、1995年兵庫県南部地震の観測記録に対して、提案した質点系モデルを用いて、回転入力動が上部建物の非線形地震応答性状に与える影響を分析した。その主な結果として、限られた範囲ではあるが、軟弱地盤ほど、また根入れが深いほど、回転入力動の影響が大きく、基礎固定で想定した塑性率を上回る応答を示す可能性があること、特に長周期建物に対して、大きな応答塑性率を設定した場合は、回転入力動の影響により、これを上回る応答が生じる場合があり、大入力に対する応答評価に対しては回転入力動に留意する必要があること、また、根入れが深い e/r=2 の場合には、回転入力動を考慮した最大応答塑性率は、回転入力動を無視した場合や地表面入力を用いる場合等より1.5倍程度大きくなることは注目に値する。一方、地盤が固い場合は、根入れが深くても回転入力動の影響が大きくないこと等が明らかとなった。

4.2 2011年東北地方太平洋沖地震の観測記録に対する分析結果

次に、2011年東北地方太平洋沖地震の本震のK-NET古川（MYG006）における観測記録（EW成分）を用いた場合について、地震動特性の違いが応答結果に与える影響を分析した。その結果、スペクトル特性による違いが現れたが、継続時間や位相の違いによる大きな差異は本検討範囲内では認められなかった。なお、これは1地震波に限られた検討結果であるため、一般性については、今後他の地震波を用いた解析を実施して検討する必要がある。

5. 結論

本論では、回転入力動が上部建物（直接基礎）の地震時非線形応答に与える影響について、Wolf[21]の改良型として、軟弱地盤にも適用できる新たな質点系モデルを提案し、限られた範囲ではあるが、建物高さや根入れ深さ等をパラメータにした非線形地震応答解析を通じた分析を行った。今後は、多層地盤や杭基礎建物、また都市域等で建物群が隣接する場合における回転入力動の建物応答への影響について検討する予定である。

（2015年8月10日原稿受理，2015年11月19日採用決定）